

## Characterization of Nylon 66 Structure from X-Ray Diffraction

J. H. DUMBLETON, D. R. BUCHANAN, and B. B. BOWLES, *Chemstrand Research Center, Inc., Durham, North Carolina 27702*

### Synopsis

A description of methods available for the determination of structural parameters in nylon 66 is given for both wide- and small-angle x-ray diffraction. The methods are applied to a series of drawn nylon 66 fibers, and the results indicate that the drawing process is one of crystal slip. It is concluded that the methods of characterization give a great deal of information about the structure along the fiber axis but that methods for examining the structure perpendicular to the fiber axis give less quantitative information and new methods are desirable.

### Introduction

The properties of polymeric materials depend to a large extent on the structure produced during processing. X-ray diffraction provides a means of characterizing polymers as a step to the establishment of structure-property relationships. This paper presents a number of techniques which have been developed over the past few years to characterize nylon 66 fibers.

### Orientation

The orientation parameter of interest for fibers is the orientation of the molecular axes with respect to the fiber axis. Since the material in a fiber is divided between crystalline and noncrystalline regions, orientation factors must be obtained for both regions.

The orientation of the molecular axes in the crystalline regions may be directly obtained from measurements of the azimuthal extent of a meridional reflection<sup>1</sup> or, in principle, from measurements on several nonmeridional reflections. X-ray diffraction gives the density distribution,  $I(\varphi)$ , of plane normals (poles) at any given orientation angle  $\varphi$ , where  $\varphi$  is the angle between a pole and the fiber axis. To convert to a number distribution the intensity  $I(\varphi)$  must be multiplied by  $\sin \varphi$ . For some studies it is sufficient to use the half-width ( $\varphi_{1/2}$ ) or some other characteristic of the density distribution as a measure of orientation. However, to relate x-ray orientation determinations to those made by other techniques the use of a parameter such as  $\overline{\cos^2 \varphi}$  is required. This parameter is defined as

$$\overline{\cos^2 \varphi} = \frac{\int_0^{\pi/2} I(\varphi) \cos^2 \varphi \sin \varphi d\varphi}{\int_0^{\pi/2} I(\varphi) \sin \varphi d\varphi} \quad (1)$$

and is a weighted mean. The weights are the number of poles at any given angle,  $\varphi$ . For any arbitrary distribution of  $I(\varphi)$ ,  $\overline{\cos^2 \varphi}$  must be determined graphically or by numerical integration. However, the calculation of  $\overline{\cos^2 \varphi}$  is made easier if  $I(\varphi)$  can be represented analytically. It has been found in this laboratory that for many polymers  $I(\varphi)$  may be represented as a Gaussian curve as follows,

$$I(\varphi) = (h/\sqrt{\pi}) e^{-h^2\varphi^2} \quad (2)$$

The value of  $\overline{\cos^2 \varphi}$  is now determined entirely by  $h$  which is related to the half-width  $\varphi_{1/2}$  of  $I(\varphi)$  by the equation

$$\varphi_{1/2} = 0.833/h \quad (3)$$

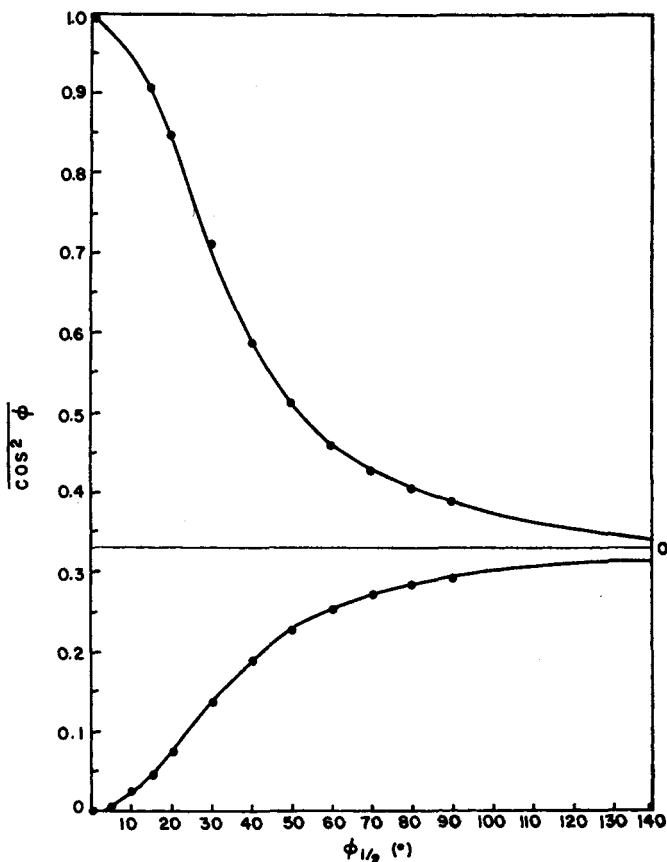


Fig. 1. Orientation parameter  $\overline{\cos^2 \varphi}$  vs. half-maximum breadth  $\varphi_{1/2}$  for a Gaussian intensity distribution.

The value of  $\overline{\cos^2 \varphi}$  has been evaluated numerically as a function of  $h$ , and a graph has been prepared of  $\overline{\cos^2 \varphi}$  against  $\varphi_{1/2}$  as shown in Figure 1. The  $\overline{\cos^2 \varphi}$  value for any reflection may be obtained from a measurement of the azimuthal half-width of the x-ray reflection. In nylon 66 the (1,3,14) reflection, which occurs at  $2\theta \cong 77^\circ$ , is suitable for orientation measurements since the normal to this plane lies only  $\sim 2^\circ$  from the molecular axis.

Stein<sup>2</sup> has shown that the birefringence of a uniaxially drawn material may be expressed as follows

$$\Delta = X f_c \Delta_c^\circ + (1 - X) f_{am} \Delta_{am}^\circ \quad (4)$$

where  $\Delta$  is the measured birefringence,  $X$  is the volume crystallinity,  $f_c$  and  $f_{am}$  are parameters defining the orientation in the crystalline and non-crystalline regions, and  $\Delta_c^\circ$  and  $\Delta_{am}^\circ$  are the birefringences of segments in the crystalline and noncrystalline regions. The orientation parameters are related to  $\overline{\cos^2 \varphi}$  as follows

$$f = 1/2 (3 \overline{\cos^2 \varphi} - 1) \quad (5)$$

$X$  may be determined from density measurements, and  $f_c$  is found from the  $\overline{\cos^2 \varphi}$  value obtained from x-ray measurements. For nylon 66 we have taken  $\Delta_c^\circ$  and  $\Delta_{am}^\circ$  as 0.073.<sup>3</sup> Therefore, a measurement of  $\Delta$  yields the noncrystalline orientation factor,  $f_{am}$ .

### Crystallinity

Density and infrared methods<sup>4</sup> of crystallinity determination in nylon 66 have been in use for some time, but no x-ray method has been successfully

TABLE I  
Density and Amorphicity Values for Drawn  
and Annealed Nylon 66 Yarns

Sample treatment	Density, g/cm <sup>3</sup>	Amorphicity index (arbitrary units)
Drawn		
1X	1.139	93
2X	1.139	93
3X	1.140	96
4X	1.142	94
5X	1.150	73
Spun yarn (heated 30 min)		
101°C	1.138	96
120°C	1.142	91
140°C	1.144	82
160°C	1.148	79
180°C	1.158	67
200°C	1.162	66
220°C	1.169	52

proposed. Crystallinity is not a well-defined property, since results from different techniques are seldom in agreement. In view of this, methods have been proposed in which relative crystallinities are determined. In one such method a point is taken on the diffraction pattern where the contribution is from the (noncrystalline) regions only.<sup>5</sup> Such a point occurs at  $2\theta = 16^\circ$  in nylon 66 as there is little crystalline contribution there. The intensity at  $2\theta = 16^\circ$ , normalized for sample mass, is a measure of the amorphicity. The total diffracted intensity may be taken as a measure of the sample mass. The amorphicity index is defined as the intensity at  $16^\circ$  ( $2\theta$ ) divided by the area under the scan.

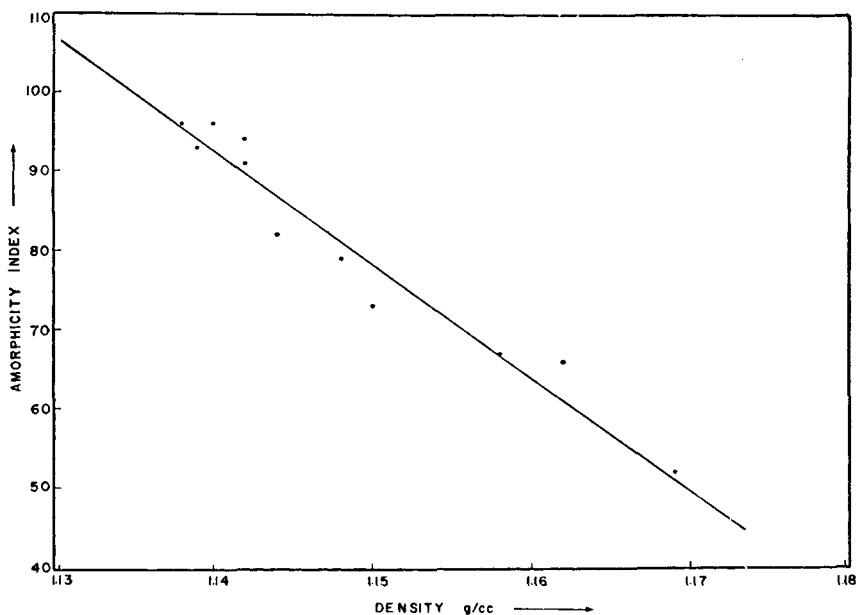


Fig. 2. Amorphicity index vs. density for nylon 66 samples of different history.

Data are given in Table I for a series of drawn and heat-treated nylon 66 yarns. A graph of amorphicity index versus density is found to be linear over the range of densities studied (see Fig. 2).

### Lateral Order

Crystallinity measurements give the ratio of the amount of crystalline to noncrystalline material present. However, examination of x-ray patterns of nylon 66 samples of different history reveals that changes other than crystallinity changes have occurred. This is especially evident for the reflections which came from planes parallel to the fiber axis, namely the (100) and (010, 110) diffraction maxima which occur on the equator of the x-ray pattern. According to Stern and Segerman<sup>6</sup> the positions of the

peaks shift with annealing temperature. Dismore and Statton<sup>7</sup> propose that the shift is best interpreted in terms of crystal imperfections. They relate this shift to the ideal crystal and calculate a crystal perfection index (CPI) using the formula:

$$\text{CPI} = \frac{(d_{100}/d_{010}) - 1}{0.189} \times 100 \quad (6)$$

where  $d_{100}$  is the interplanar spacing of the (100) planes and the  $d_{010}$  that of the (010) planes. The denominator is the corresponding value for a well-crystallized sample as reported by Bunn and Garner.<sup>8</sup>

The CPI is a measure of what is loosely called crystal perfection. It is complicated by the fact that some of the shift may be due to overlapping with nonequatorial reflections and by the presence of noncrystalline background below the equatorial doublet.

### Crystal Size and Lattice Distortion

The width of a crystalline diffraction peak is a function of crystal size and lattice distortion. The integral breadth of the lattice distortion profile is<sup>9</sup>

$$B_D = 4 e (\sin \theta / \lambda) \quad (7)$$

where  $e$  ( $\propto \delta d_{hkl}/d_{hkl}$ ) is a measure of the maximum lattice distortion. The integral breadth of the crystal size profile may be taken as the Scherrer equation<sup>9</sup>

$$\beta_s = C/L_{hkl} \quad (8)$$

where  $C$  is a constant related to crystal shape and to the way in which  $\beta_s$  and  $L_{hkl}$  are defined. If  $\beta$  is an integral breadth and the crystals are roughly cubic or spherical in shape, then  $C$  is unity. It has been found that the broad profiles generally found in polymers may be approximated as Gaussian curves. On the basis of this assumption, the combination of size and distortion broadening leads to a profile of breadth  $\beta$  given by

$$\beta^2 = (1/L_{hkl}^2) + 16e^2(\sin^2 \theta / \lambda^2) \quad (9)$$

If two true orders of reflection are observable, then the size and distortion components may be separated. Since it is difficult to observe even two orders the best course is to consider reflections which have different  $d$  spacings but which make the same or approximately the same angle to the fiber axis. In nylon 66 the equatorial reflections overlap one another, and the noncrystalline background is difficult to determine. It is then natural to look for reflections which are from planes perpendicular to the fiber axis. In nylon 66, the (015) and (1,3,14) planes are suitable for measurement. The (015) plane occurs at  $2\theta = 26.6^\circ$  and its normal makes an angle of  $15^\circ$  to the fiber axis, while the corresponding values for the (1,3,14) plane are  $2\theta = 77.1^\circ$  and  $2^\circ$ .

The integral breadth obtained experimentally  $\beta_E$  must be corrected for instrumental broadening. If the true and the instrumental profiles  $\beta_I$  are assumed to be Gaussian, which again is a good approximation, then

$$\beta^2 = \beta_E^2 - \beta_I^2 \quad (10)$$

The value of  $\beta_I$  is obtained from broadening measurements on the diffraction peaks of a sample consisting of large crystals which themselves would give negligible broadening.

### Superstructure

The data obtained from a small-angle (i.e., scattering angles less than  $\sim 2^\circ$ ) x-ray scattering experiment on a polymer fiber usually show the presence of continuous scattering near the incident beam and "peaked" scattering at higher scattering angles. One commonly observed aspect of the scattering parallel to the fiber axis is the long period, a maximum in the overall scattering curve which, in polymers, normally occurs at angles corresponding to distances in the range 50–300 Å. The distance corresponding to the long period is commonly taken to represent the repeat of a structural feature along the fiber axis. This distance is often observed to increase when a fiber is drawn or annealed, and thus is an indicator of structural changes in the fiber. Although the observed long period may serve to characterize a particular fiber, long periods alone do not consistently seem to predict other fiber characteristics such as mechanical properties. Some attempts<sup>10</sup> have been made to combine long period data with minimum crystal sizes obtained from meridional wide-angle diffraction data, but there are several inconsistencies in that approach: the crystallite size calculated from wide angle diffraction was not corrected for lattice distortion broadening and, in addition, even a correctly computed size is normally a weight-average size, while it is not clear what kind of averaging process is reflected by the long period.

Recently, Tsvankin<sup>11</sup> calculated theoretical scattering curves based on the following model: (1) a fiber is composed of parallel fibrils with regions of higher and lower electron densities alternating regularly along the fibril axis: the regions of lower electron density correspond to "amorphous" segments and those of higher electron density to crystals; (2) the distribution of crystallite sizes (as projected on to the fiber axis) is assumed to be rectangular with limits  $a - \Delta$  and  $a + \Delta$ , where  $a$  is the mean (number-average) crystal length, and a long period  $c$  is defined as the mean projected distance between crystallite centers (due to the range of sizes present  $c$  is not the same distance as the measured long period); (3) a transition region of intermediate electron density is assumed to exist at the edge of each crystallite.

The experimental data may be analyzed from a long-period measurement and from the half-width of the meridional small-angle maximum providing the following conditions are specified: the length of the transition

region relative to the crystal size and the dispersion of the crystal lengths about the mean. Tsvankin showed that the results were insensitive to values of the ratio of the length of the transition region to crystal size in the range 0.2–0.3 (consequently 0.2 has been used in the present work). In the course of testing the Tsvankin procedure it was found that, for a series of drawn nylon 66 yarns, the mean crystallite length  $a$  was constant for values of the dispersion ratio from 0.1 to 0.5, although the “amorphous” length  $l$ , ( $a + l = c$ ) and the mean long period  $c$ , varied greatly. It appears that a number-average crystal size can be calculated regardless of assumptions about the dispersion ratio.

Strictly speaking, the Tsvankin treatment may be applied only to perfectly oriented fibers. In practice it is found that fibers of draw ratio greater than  $2\times$  are sufficiently well oriented to be considered by the Tsvankin approach.

Although no maxima are seen in directions perpendicular to the fiber axis, it is found that the lateral extent of the small angle maximum is dependent on the thermal and drawing history of the fiber. If the fibrils scattered as independent entities, the lateral width of the small-angle maximum would be a measure of the diameter of a fibril. Complicating factors arise in this assumption<sup>12</sup> but since the variables affecting the lateral width are not known, it is sufficient to use the simple assumption that the width gives an effective fibril size.

### Experimental

A series of nylon 66 yarns drawn over a hot block at 180°C was used to illustrate the various methods of x-ray characterization. Each sample was wound on an aluminum sample holder in such a manner that the individual strands were as parallel as possible. Wide-angle data were obtained in transmission by using an automated x-ray diffractometer with point counting for 10,000 counts or 10 min per point, whichever occurred first. Ni-filtered  $\text{CuK}\alpha$  radiation at 35 kV and 20 ma was used, and the diffracted beam was detected by a scintillation counter in conjunction with a pulse height analyzer.

The CPI was obtained from an equatorial scan over the range 5–35° ( $2\theta$ ). The crystallinity was determined from a  $2\theta$  scan over the same angular range but with the specimen rotating to include all the scattered intensity. The widths of the (015) and (1,3,14) reflections were obtained from  $2\theta$  scans in the range 23–33° ( $2\theta$ ) and 72–84° ( $2\theta$ ), respectively.\* The orientation of the crystals was obtained from an azimuthal scan of the (1,3,14) reflection. The orientation of the amorphous regions was obtained from birefringence, density crystallinity, and the orientation of the crystalline regions, as shown in eq. (4).

Small-angle determinations of the long period were made with slit collimation on a Kratky camera by using photographic techniques. The

\* The instrumental broadening was obtained from measurements of peak width on a sample of hexamethylenetetramine.

photographs were scanned with a Joyce-Loebel microdensitometer. The long period and the half-width of the diffraction maximum were obtained from the scans. The lateral extent of the meridional maximum was obtained from photographs taken with pinhole collimation.

No comment on the treatment of the data is required except in the case of the treatment of the small-angle maximum. It was previously mentioned that the crystal sizes are independent of the crystal dispersion. Crystal sizes obtained from wide-angle and small-angle data were compared to yield the information that the ratio of weight-average to number-average size is in the range 1.1–1.2. For a crystal size of 50 Å and a rectangular size distribution this ratio implies that the crystal dispersion lies in the range 0.4–0.8. Accordingly a value of 0.5 was used in the remainder of the analysis. It may be noted that Zubov and Tsvankin<sup>13</sup> based their analysis of polypropylene and nylon 6 data on a ratio of 0.2–0.3.

### Results

From the data in Table II it is seen that the orientation of both the crystalline and amorphous regions increase with draw ratio. The orientation of the crystalline regions is approaching the limit of unity at the highest draw ratio of 5×, while the orientation of the amorphous regions is always lower than that in the crystalline regions. In addition, it will be noted that the crystals have almost reached the maximum orientation at a draw ratio of 2×. The orientation in the amorphous regions continues to increase even at the 5× draw ratio.

TABLE II  
Lateral Order and Orientation Data for Nylon 66 Tire Yarns

Sample draw ratio	CPI	$1/B_{SA}$ , Å <sup>a</sup>	Amorphicity index	$f_c$	$f_{am}$
1×	0.59	—	93	0	0
2×	0.58	27 <sup>b</sup>	93	0.891	0.368
3×	0.57	27	96	0.928	0.483
4×	0.57	28	94	0.943	0.528
5×	0.59	33	73	0.963	0.591

<sup>a</sup>  $B_{SA}$  is the width of the small-angle maximum parallel to the equator expressed in reciprocal Å.

<sup>b</sup> Slight tendency towards an arc in the small angle maximum.

From the data in Table III it is seen that the radial integral breadths for both (015) and (1,3,14) decrease with drawing. The integral breadth for (015) could not be measured below draw ratios of 3×; that for (1,3,14) was difficult to measure accurately at any draw ratio due to a pronounced asymmetry in the profile which was apparently caused by overlap with other 14th layer line diffraction planes [principally (0,3,14)]. This asymmetry becomes very pronounced at low draw ratios. The integral breadths shown for (1,3,14) are based on the following construction. The (1,3,14)



TABLE III  
Drawn Nylon 66 Tire Yarn Wide-Angle Diffraction

Sample draw ratio	Integral breadth of (015), $\text{\AA}^{-1}$	Integral breadth of (1,3,14), $\text{\AA}^{-1}$	Apparent weight-average size from (015), $\text{\AA}$	"True" weight-average size in approximate direction of the fiber axis, $\text{\AA}$	Maximum lattice distortion in approximate direction of the fiber axis, %	Number-average size obtained from small-angle data, $\text{\AA}$
1X	—	—	—	—	—	41
2X	—	0.02380	—	49	0.78	44
3X	0.01906	0.02147	52	57	0.78	51
4X	0.01724	0.02071	58	66	0.90	56
5X	0.01448	0.01751	59	79	0.78	73

profile from the 5 $\times$  sample is nearly symmetric with a pronounced maximum at  $2\theta = 77.1^\circ$  (the theoretical value for this maximum based on the unit cell of Bunn and Garner<sup>8</sup> is  $77.7^\circ$ ). Each of the (1,3,14) profiles was terminated at  $77.1^\circ$ , and the integral breadth of the low-angle portion of the profile was measured. Twice this figure is shown in Table III.

As a result of these uncertainties the lattice distortions shown in Table III are only approximate, although the near constancy with draw ratio is probably an accurate conclusion. The weight-average crystal sizes, on the other hand, are not greatly affected by uncertainties in the (1,3,14) integral breadth, as evidenced by their similarity to the "apparent" crystallite sizes calculated from (015) data alone, for which the effects of lattice distortion are ignored. The weight-average crystallite size for the 2 $\times$  sample was obtained from the (1,3,14) profile alone, for which a lattice distortion of 0.78% was assumed.

The amorphicity index values are shown in Table II. The more crystalline the sample the lower should be the amorphicity index. It will be seen that the 2 $\times$ -4 $\times$  yarns all have the same crystallinity but that there is an increase in crystallinity for the 5 $\times$  sample. The crystal perfection index, however, is constant throughout the series, which indicates that there is no change in perfection in the direction perpendicular to the fiber axis.

The results of the analysis of the small angle data for the drawn series are shown in Table IV. On drawing the observed long period increases and there is a concomitant decrease in the half-width of the maximum. Even the spun (1 $\times$ ) sample was consistent with the rest of the group in these respects, although, since this sample was unoriented the Tsvankin analysis may not be directly applicable. The mean long periods  $c$  are all smaller than the observed long periods but show a similar increase on drawing as do the mean crystallite lengths. The mean amorphous lengths decrease slightly on drawing. The one-dimensional crystallinities also increase on drawing; they are considerably higher than density crystallinities (Table I), which are near 50%.

The findings that the "amorphous" regions maintain a nearly constant length of drawing are consistent with those of Statton<sup>10</sup> although the sizes found here of 16-20 Å are much smaller than those deduced by Statton, who found 30-40 Å. The principal cause of this discrepancy lies in the interpretation of the data. If, as did Statton, only "apparent" crystallite sizes derived from the (015) peak shape and long period measurements are considered, then amorphous lengths of 29, 30, and 41 Å are found for the 3 $\times$ , 4 $\times$ , and 5 $\times$  samples.

An amorphous length of 16-20 Å, in addition to its resemblance to the  $c$ -axis length of the nylon 66 unit cell, is also within the range of likely distances of closest approach for the ordered regions of two folded-chain lamellae in which the folds involve seven covalent bonds. This distance is also comparable to Zaukelies' estimates<sup>14</sup> of 1.8 vacant unit cells per fold and 0.9 vacant unit cells per chain end as an explanation of the difference between the theoretical and observed densities in nylon 66. Zaukelies,

TABLE IV  
Drawn Nylon 66 Tire Yarn Small-Angle Meridian Scattering

Sample draw ratio	Measured long period, Å	Half-width of small-angle maximum, Å <sup>-1</sup>	Mean long period, Å	Mean crystal size along fiber axis from Tsvankin treatment <i>a</i> , Å	Mean amorphous length along the fiber axis <i>l</i> , Å	One-dimensional crystallinity along the fiber axis <i>a</i> /( <i>a</i> + <i>l</i> )
1X	72	0.00909	62	41	21	0.66
2X	73	0.00862	62	44	18	0.71
3X	81	0.00714	67	51	16	0.83
4X	88	0.00657	72	56	16	0.82
5X	110	0.00500	90	73	17	0.82

however, assumes an average chain length between folds of 50 unit cells while our data indicates chain lengths of only 3–5 unit cells. On this basis defective regions of dislocations and grain boundaries seem more likely than vacancies of this magnitude.

The weight-average sizes  $L$  may be compared with the number-average sizes  $a$  obtained from the small angle data. The ratio of weight-average to number-average size is consistently 1.1–1.2.

The widths of the small-angle maximum parallel to the equator decrease as a function of draw ratio indicating an increase in perfection of the structure in the direction perpendicular to the fiber axis, whereas CPI remains unchanged.

### Discussion

The results indicate that the drawing of nylon 66 fibers does not involve the formation of new regions of order but rather the rearrangement of regions existing in the spun fiber. The methods of characterization show that the orientation increases on drawing with almost all the orientation being achieved by a draw ratio of  $2\times$ . This observation indicates that drawing proceeds by a slip mechanism. The growth of the crystallites in the direction of the fiber axis on drawing, together with the nearly constant length of the noncrystalline segments, implies that the material for growth is taken from outside the fibril.

The information regarding changes perpendicular to the fiber axis is much less complete although the small angle data do indicate an increase in perfection of the structure. Further information on the structure perpendicular to the fiber axis is needed. Unfortunately, the separation of the effects of small crystallite size and lattice distortion on the breadths of the equatorial diffraction maxima has not been accomplished for nylon 66, due to the considerable experimental difficulties involved.

### References

1. P. H. Hermans, *Physics and Chemistry of Cellulose Fibres*, Elsevier, Amsterdam, 1949.
2. R. S. Stein and F. H. Norris, *J. Polym. Sci.*, **21**, 381 (1956).
3. M. F. Culpin and K. W. Kemp, *Proc. Phys. Soc.*, **69**, 1301 (1957).
4. H. W. Starkweather and R. E. Moynihan, *J. Polym. Sci.*, **22**, 363 (1956).
5. P. H. Hermans and A. Weidinger, *J. Polym. Sci.*, **4**, 135 (1949).
6. P. G. Stern and E. Segerman, *Nature*, **210**, 1258 (1966).
7. P. F. Dismore and W. O. Statton, in *Small Angle Scattering From Fibrous and Partially Oriented Systems* (*J. Polym. Sci. C*, **13**), R. H. Marchessault, Ed., Interscience, New York, 1966, p. 133.
8. C. W. Bunn and E. V. Garner, *Proc. Roy. Soc. (London)*, **A189**, 39 (1947).
9. D. R. Buchanan and R. L. Miller, *J. Appl. Phys.*, **37**, 4003 (1966).
10. W. O. Statton, *J. Polym. Sci.*, **41**, 143 (1959).
11. D. Ya. Tsvankin, *Polym. Sci. USSR*, **6**, 2304, 2310 (1964).
12. A. Guinier, *Ann. Phys. (Paris)*, **12**, 90 (1939).
13. Yu. A. Zubov and D. Ya. Tsvankin, *Polym. Sci. USSR*, **6**, 2358 (1964).
14. D. A. Zaukelies, *J. Appl. Phys.*, **33**, 2797 (1962).

Received January 22, 1968

Revised March 7, 1968